

Drift estimation in stochastic flows using kernel integral operators

Suddhasattwa Das*

April 19, 2024

Abstract

A stochastic differential equation (SDE) describes a motion in which a particle is governed simultaneously by the direction provided by a vector field / drift, and the scattering effects of white noise. The resulting motion can only be described as a random process instead of a solution curve. Due to the non-deterministic nature of this motion, the task of determining the drift from data is quite challenging, since the data does not directly represent the directional information of the flow. This paper describes an interpretation of vector field as a conditional expectation, which makes its estimation feasible via kernel-integral methods. It presents a numerical procedure based on kernel integral operators, that computes this expectation. In addition, some techniques are presented which can overcome the challenge of dimensionality if the SDE's carry some structure enabling sparsity.

Key words. Markov kernel, statistical denoising, compact operators, RKHS

AMS subject classifications. 46E27, 46E22, 62G07, 62G05

arXiv:2404.10698v2 [math.DS] 18 Apr 2024

1 Introduction.

This article presents a convergent and consistent technique for estimating the drift in stochastic differential equations (SDE), from data collected from observations of the system at fixed sampling intervals of Δt . We consider a general d -dimensional SDE :

$$dX(t) = V(X(t)) + G(X(t)) dW^t. \quad (1)$$

Due to the stochasticity created by the white noise, the solutions $X(t)$ to an SDE is a Markov process instead of being a curve (1; 2). In addition if the following assumption holds :

Assumption 1. *The SDE (1) has a stationary probability measure ν .*

Then $X(t)$ is a stationary Markov process as well. One of the basic tenets of the theory of Markov processes is that the derivative of the conditional expectations of a stationary Markov process is provided by the generator \mathcal{L} (3, Cor 160) :

$$\frac{d}{ds} \Big|_{s=t} \mathbb{E}(\phi(X(s)) | X(t)) = \mathcal{L}X(t), \quad \forall \phi \in \text{dom}(G). \quad (2)$$

In the case of an SDE, the generator is the forward Kolmogorov operator \mathcal{L} . Its action on a C^2 function g is given by :

$$(\mathcal{L}g)(X, t) := \sum_{i,j=1}^{2N} \frac{\partial^2}{2\partial X_i \partial X_j} (\langle \{F_{diff}\}_i, \{F_{diff}\}_j \rangle g(X, t)) - \sum_{i=1}^{2N} \frac{\partial}{\partial X_i} (\{F_{drift}\}_i g(X, t)). \quad (3)$$

*Department of Mathematics and Statistics, Texas Tech University, Texas, USA

Of special interest to us is the particular instance of (2) when $\phi = \text{Id}_{\mathbb{R}^d}$ and $t = 0$. It takes the form

$$\lim_{t \rightarrow 0^+} \frac{1}{t} \mathbb{E} (X(t, x_0) - x_0) = (\mathcal{L} \text{Id}_{\mathbb{R}^d})(x_0) = V(x_0). \quad (4)$$

This is the main mathematical principle we rely on in developing our numerical technique. In fact we use a third order version (4, Eqn 21) of (4) given by

$$\Delta t V(x_0) = 18 \mathbb{E} (X(\Delta t, x_0) - x_0) - 9 \mathbb{E} (X(2\Delta t, x_0) - x_0) + 2 \mathbb{E} (X(3\Delta t, x_0) - x_0) + O(\Delta t^3). \quad (5)$$

The approximation (5) is a consequence of the Taylor series for the Kolmogorov operator :

$$\mathbb{E} [(\phi(X_{t+\Delta t}) - \phi(X_t)) | X_t] = \sum_{n=1}^k \frac{1}{n!} \Delta t^n (\mathcal{L}^n \phi)(X_t) + O(\Delta t^k), \forall \phi \in C^{2k}(\mathbb{R}^d). \quad (6)$$

While the connections between the terms of an SDE and the properties of the stochastic process it generates is well known, the task of numerical estimation remains challenging. We are interested in the following situation :

Assumption 2. *There is sampling interval $\Delta t > 0$, and an initial state x_0 and a collection of N pairs of points*

$$\{(X((t_n + 1)\Delta t, x_0), X(t_n \Delta t, x_0)) : t_1 < t_2 < \dots\} \quad (7)$$

in which each pair are two points of a typical trajectory starting from x_0 , sampled at a time interval of Δt .

We can now specify our goal to be an estimation of the drift V from (1), assuming Assumptions 1 and 2. While there has been many diverse and reliable techniques for approximating the drift for ODEs (e.g. 5; 6; 7; 8), it is still a challenge (9) to develop a technique that fulfills the following criterion :

- (i) is nonparametric;
- (ii) is convergent with data;
- (iii) does not assume a prior distribution;
- (iv) is adaptable to high dimensional systems.

Some notable techniques which utilize parametric forms is for Langevin equations (10; 11) and electrical systems (12). Effective nonparametric techniques have been built (13) which are well suited to sparse sampling but are rely on the assumption of prior distributions.

The technique that we develop utilizes the following observation

Lemma 1.1. *Under Assumptions 1 and 2, there is a measure μ on $\mathbb{R}^d \times \mathbb{R}^d$ such that*

- (i) *the data from (7) is equidistributed according to μ ;*
- (ii) *the projection of μ to the first coordinate equals ν ;*
- (iii) *The drift of the SDE (1) is given by*

$$V = \mathbb{E}_\mu (\text{proj}_2 | \text{proj}_1) \quad (8)$$

The technique that we develop essentially approximates the identity in (8). The left hand side (LHS) is approximated using (8), and the right hand side RHS using an operator theoretic tool from (14). We

show in Section 3 how our techniques extend easily to high dimensional systems, under certain conditions of sparsity.

It is worth mentioning that there are several notable nonparametric methods which are theoretically sound, but lack the simplicity of the method we present. Sechi (15) has proposed a technique of approximating the generator of the Markov process created by the SDE. Another interesting theoretical tool is the use of the Stochastic Itô–Taylor expansion (16), but it has only been adapted to one-dimensional stochastic processes. One of the classical approaches is using finite differences to reconstruct joint probability density functions (e.g. 17). However this technique is very sensitive to undersampling and time step, and hence faces challenges in dimensions 3 or more. Another major theoretical approach to the drift estimation problem was proposed by Banon (18). The drift is estimated from the stationary density of the process, and the technique has been shown to be convergent under certain set of conditions.

Outline. This completes a description of the problems we aim to solve, and the underlying mathematical principles. We next present in Section 2 a numerical recipe for implementing the conditional expectation route to drift estimation. We then show in Section 3 how our techniques extend easily to high dimensional systems, under certain conditions of sparsity. We next apply these numerical procedures to some examples in 4. We end with some discussions in Section 5.

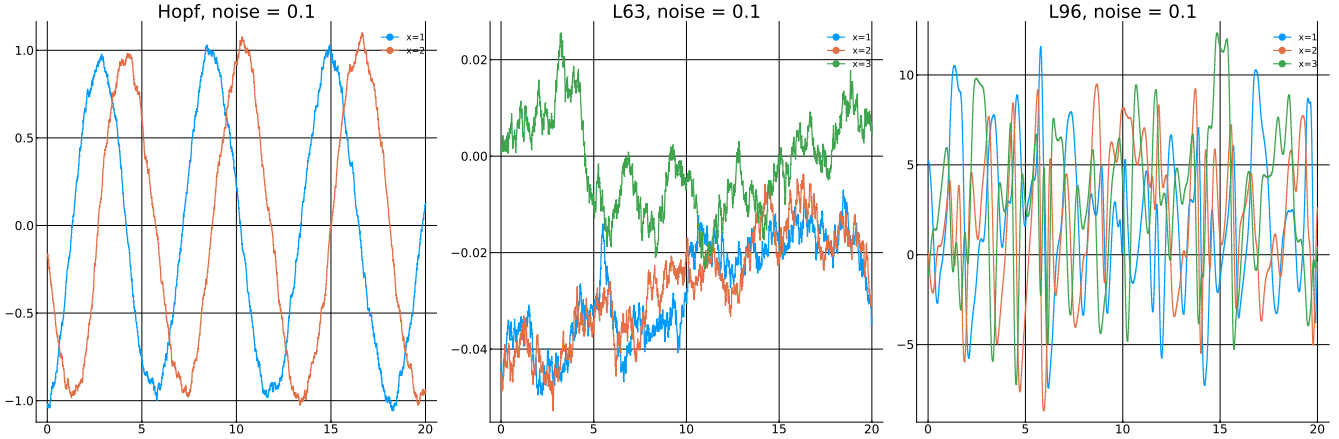


Figure 1: Orbits from SDEs. The three plots show a sample path of SDEs, in which the drifts are the Hopf oscillator (18), Lorenz-63 system (17) and the Lorenz 96 system (19). The SDEs have a diagonal diffusion term given by (20). The parameters of the experiments are provided in Table 1. The legends indicate the index of the coordinates being plotted. The paper presents a numerical method for extracting the drift from such SDE generated timeseries. The results of the reconstruction have been displayed in Figures 3, 2, and 5 respectively. To further assess the accuracy of the methods, we compared the orbits generated by the true and estimated vector fields in Figures 6 and 7 respectively.

2 The technique.

Our technique makes multiple and different uses of kernels and kernel integral methods. A *kernel* on a space \mathcal{X} is a bivariate function $k : \mathcal{X} \times \mathcal{X} \rightarrow \mathbb{R}$, which is supposed to be a measure of similarity between points on \mathcal{X} . Bivariate functions such as distance and inner-products are examples of kernels. Kernel based methods offer a non-parametric approach to learning, and have been used with success in many diverse fields such as spectral analysis (19; 20), discovery of spatial patterns (e.g. 21; 22), and the discovery of periodic and chaotic components of various real world systems (e.g. 23; 24), and even abstract operator valued measures

(25). We shall use the widely used *Gaussian* kernels, defined as

$$k_{\text{Gauss},\delta}(x, y) := \exp\left(-\frac{1}{\delta} \text{dist}(x, y)^2\right), \quad \forall x, y \in X. \quad (9)$$

Gaussian kernels have the important property of being *strictly positive definite*, which means that given any distinct points x_1, \dots, x_N in \mathcal{X} , numbers a_1, \dots, a_N in \mathbb{R} , the sum $\sum_{i=1}^N \sum_{j=1}^N a_i a_j k(x_i, x_j)$ is non-negative, and zero iff all the a_i -s are zero. An important kernel for us will be a Markov normalized version of the Gaussian kernel (9). Given a measure β on \mathcal{X} and a bandwidth parameter $\delta > 0$, define

$$k_{\text{Gauss},\delta}^{\text{symm},\beta} : \mathcal{X} \times \mathcal{X} \rightarrow \mathbb{R}, \quad k_{\text{Gauss},\delta}^{\text{symm},\beta}(x, x') := k_{\text{Gauss},\delta}(x, x') / \int_{\mathcal{X}} k_{\text{Gauss},\delta}(x, x'') d\beta(x''). \quad (10)$$

Closely associated to kernels are kernel integral operators (k.i.o.). Now suppose that \mathcal{X} is a C^r -smooth manifold. Given a probability measure ν on \mathcal{X} , one has an integral operator associated to a continuous kernel k , defined as

$$K^\nu : L^2(\nu) \rightarrow C^r(\mathcal{X}), \quad (K^\nu \phi)(x) := \int_{\mathcal{X}} k(x, y) \phi(y) d\nu(y).$$

If the kernel k is C^r , then its image set will also be C^r functions. For this reason, k.i.o.-s are also known as smoothing operators. In fact, under mild assumptions, k.i.o.-s embed functions in $L^2(\nu)$ into function spaces of higher regularity, called *RKHS*. Recall that a kernel k is *symmetric* if for every $x, x' \in X$, $k(x, x') = k(x', x)$. Symmetric kernels allow the use of tools from RKHS theory, which we review shortly.

RKHS. A reproducing kernel Hilbert space or *RKHS* is a Hilbert space of continuous functions, in which pointwise evaluations are bounded linear functionals. Any continuous symmetric, strictly positive definite kernel k (such as (21)) induces an RKHS which contains linear sums of the form $\sum_{n=1}^N a_n k(\cdot, x_n)$, in which the inner product is given by

$$\left\langle \sum_{n=1}^N a_n k(\cdot, x_n), \sum_{m=1}^M b_m k(\cdot, y_m) \right\rangle = \sum_{n=1}^N \sum_{m=1}^M a_n^* b_m k(x_n, y_m).$$

The full details of the construction of this space \mathcal{H} can be found in any standard literature (e.g. 26). The functions $k(\cdot, x_n)$ are called the *sections* of the kernel k . The kernel sections are members of the RKHS and span the RKHS. One of the defining properties of RKHS is the *reproducing* property :

$$\langle k(\cdot, x), f \rangle = f(x), \quad \forall x \in X, \forall f \in \mathcal{H}.$$

When an RKHS is used as the hypothesis space in a learning problem, the target function is assumed to be a finite sum $\sum_{n=1}^N a_n k(\cdot, x_n)$ of the kernel sections. Let ν be any probability measure on X , and K^ν be the kernel integration operator associated to k and ν . Then it is well known that the image of K^ν lies in \mathcal{H} . We denote this image as \mathcal{H}_ν . For example, let ν be a discrete measure $\nu = \sum_{n=1,2,\dots} w_n \delta_{x_n}$, i.e., an aggregate of Dirac-delta measures supported on discrete points x_n along with weights $w_n > 0$ which sum to 1. Then \mathcal{H}_ν is precisely the span of the kernel sections $\{k(\cdot, x_n) : n = 1, \dots, N\}$.

This completes a brief description of the theoretical grounds of our numerical methods. We present our first algorithm from (14) for computing conditional expectation from data.

Algorithm 1. *RKHS representation of conditional expectation.*

- **Input.** A sequence of pairs $\{(x_n, y_n) : n = 1, \dots, N\}$ with $x_n \in \mathbb{R}^d$ and $y_n \in \mathbb{R}$.
- **Parameters.**

1. Choice of RKHS kernel $k : \mathbb{R}^d \times \mathbb{R}^d \rightarrow \mathbb{R}^+$.

2. Smoothing parameter $\epsilon_1 > 0$.
3. Sub-sampling parameter $M \in \mathbb{N}$ with $M < N$.
4. Ridge regression parameter δ .

• **Output.** A vector $\bar{a} = (a_1, \dots, a_M) \in \mathbb{R}^M$ such that

$$(E^\alpha f)(x) \approx \sum_{m=1}^N a_m k(x, x_m), \quad \forall x \in \mathbb{R}^d.$$

• **Steps.**

1. Compute a Gaussian Markov kernel matrix using (10) :

$$[G_{\epsilon_1}] \in \mathbb{R}^{N \times N}, \quad [G_{\epsilon_1}]_{i,j} = k_{\text{Gauss}, \delta}^{\text{symm}, \beta}(x_i, x_j). \quad (11)$$

2. Compute a Markov kernel $[P] \in \mathbb{R}^{N \times N}$ as $[P]_{i,j} := p(x_i, x_j)$
3. Compute the kernel matrix $[K] \in \mathbb{R}^{N \times M}$ as $[K]_{i,j} = k(x_i, x_j)$.
4. Find a vector $\bar{a} \in \mathbb{R}^M$ as the δ -regularized least-squares solution to the equation

$$[P][K]\bar{a} = [P][G_{\epsilon_1}]\bar{y}. \quad (12)$$

Algorithm 1 has two components, the choice of an RKHS kernel, and the creation of a Markov kernel which approximates the smoothing operator. We usually choose p to be the Markov normalized Gaussian kernel from (10). The algorithm is convergent in the following sense :

Lemma 2.1. (14, Thm 2) Suppose there is a probability space (Ω, μ) and two measurable functions $X : \Omega \rightarrow \mathbb{R}^d$ and $Y : \Omega \rightarrow \mathbb{R}$. Suppose that the sequence $\{(x_n, y_n)\}_{n \in \mathbb{N}}$ is equidistributed with respect to some measure on $\mathbb{R}^d \times \mathbb{R}$. Let \bar{f} denote the conditional expectation $\mathbb{E}_\mu(Y|X)$. Suppose the kernel k in Algorithm 1 is derived from a Gaussian kernel of bandwidth ϵ_2 which is an integer multiple of ϵ_1 . Then the output \bar{a} of Algorithm 1 satisfies :

$$\lim_{M \rightarrow \infty} \lim_{N \rightarrow \infty, \delta \rightarrow 0^+} \left\| \sum_{n=1}^N a_n k(\cdot, x_n) - \mathcal{G}_{\epsilon_1}^\mu \bar{f} \right\|_{\mathcal{H}} = 0, \quad \lim_{\epsilon_1 \rightarrow 0^+} \left\| \mathcal{G}_{\epsilon_1}^\mu \bar{f} - \bar{f} \right\|_{L^2(\nu)} = 0. \quad (13)$$

Lemma 2.1 is in fact stated in more generality. It holds true as long the smoothed function $\mathcal{G}_{\epsilon_1} \bar{f}$ lies in the RKHS created by k . Suppose \tilde{k} is a Gaussian kernel whose bandwidth is an integer m multiple of ϵ_1 . Then the corresponding integral operators satisfy $\tilde{K} = \mathcal{G}_{\epsilon_1}^m$, from the convolution law for Gaussian kernels (e.g. 27). The same would hold true for a kernel k which is derived from \tilde{k} . The particular derivation we have in mind is a similarity transform, as shown in (22) later.

We fix some notation before describing Algorithm 2. Given any $d \times M$ matrix A , we use A_i and A^j to denote its i -th column vector and j -th row vector respectively. Given a sequence $\{z_n\}_{n=1}^N$ of d -dimensional vectors, we use $\{z_n^{(i)}\}_{n=1}^N$ to denote the 1-dimensional timeseries created by extracting the i -th coordinate from these vectors. We now present how Algorithm 1 can be used to estimate the drift from an SDE orbit.

Algorithm 2. Drift estimation as a conditional expectation

- **Input.** Timeseries $\{x_n\}_{n=1}^N$ in \mathbb{R}^d ; a sampling interval Δt .
- **Parameters.** Same as Algorithm 1.

- **Output.** A matrix $A \in \mathbb{R}^{d \times M}$ representing a vector field

$$\hat{V}(X) \approx \sum_{m=1}^M A_m k(x, x_m), \quad \forall x \in \mathbb{R}^d.$$

- **Steps.**

1. Compute

$$z_n = \frac{1}{\Delta t} [18x_{n+1} - 9x_{n+2} + 2x_{n+3} - 11x_n], \quad \forall n \in 1, \dots, N-1.$$

2. For each $i \in 1, \dots, d$, pass the timeseries $\left\{ \left(x_n, z_n^{(i)} \right) \right\}_{n=1}^N$ into Algorithm 1, along with the rest of the parameters.

3. Store the result in a m -dimensional column vector $\tilde{a}^{(i)}$.

4. Compute the $d \times M$ matrix A such that

$$A^T = [\tilde{a}^{(1)}, \tilde{a}^{(2)}, \dots, \tilde{a}^{(d)}].$$

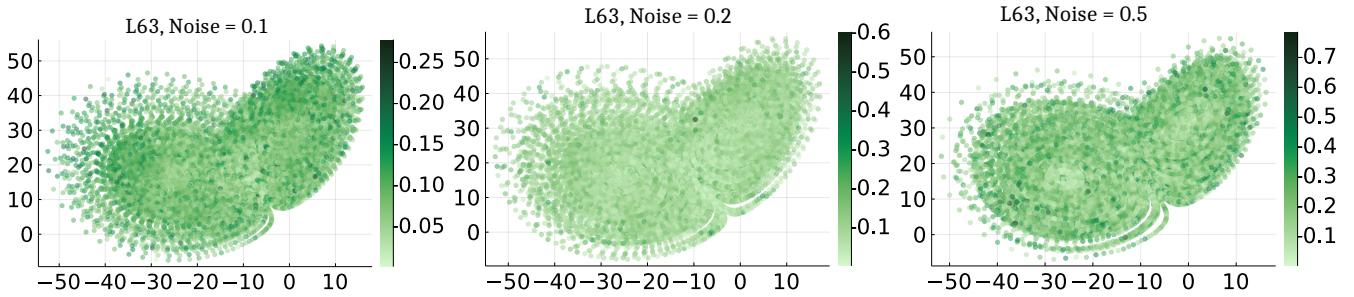


Figure 2: Estimating the drift in a stochastic Lorenz 63 model. The top left figure shows a trajectory created by simulating the SDE. The remaining pictures show the error plot in computing each of the coordinates of the vector field (17).

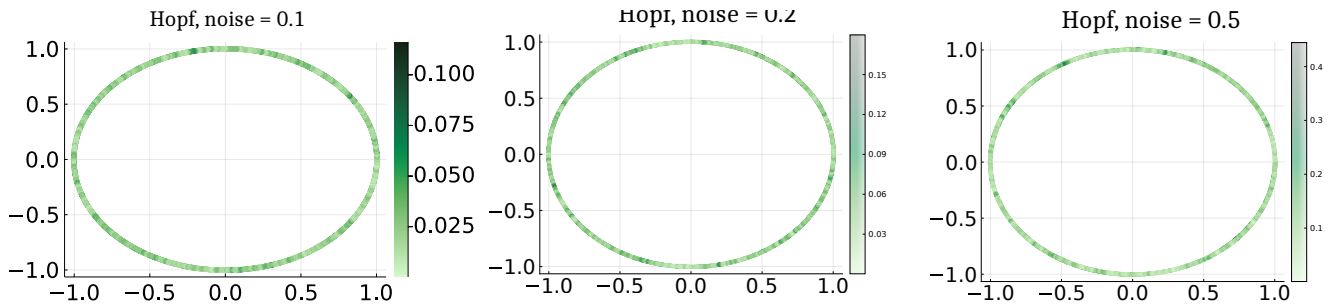


Figure 3: Estimating the drift in a stochastic version of the Hopf oscillator (18). The figures carry the same interpretation as Figure 2.

The convergence of Algorithm 2 is guaranteed by Lemma 2.1 and (8).

3 High dimensional and missing data.

We have seen in Algorithm 1 that the conditional expectations are approximated by averaging with respect to empirical measures. Empirical measure is the measure directly available to the algorithm. It is the discrete

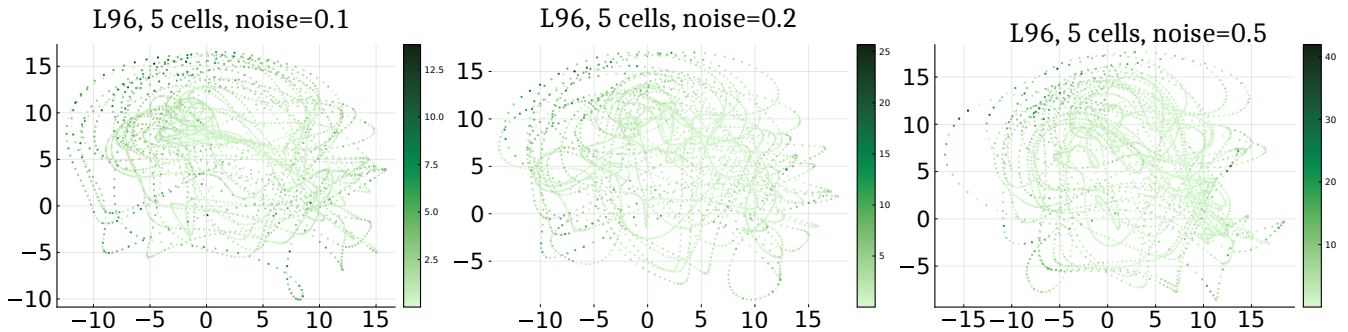


Figure 4: Estimating the drift in a stochastic version of the L96 system (19) with 5 oscillators. The figures carry the same interpretation as Figure 2.

probability measure whose supports are the data points. The key principle behind the technique is that the empirical measure provides a weak approximation of the unknown measure μ . One of the major challenges of all numerical methods is undersampling in high dimensions. If the dimension d of the phase space is large, then this approximation may not be good enough to be within a reasonable degree of accuracy.

We now examine a technique for high dimensional SDEs, in which each component of vector field is the same functional unit depending on a few other coordinates. More precisely, we assume

Assumption 3. *Given the SDE (1), there is an integer $m \ll d$, a function $\tilde{V} : \mathbb{R}^d \rightarrow \mathbb{R}$, and for each $i \in \{1, \dots, d\}$ a collection $\text{Left}(i)$ of m coordinates $(k_{i,1}, \dots, k_{i,m}) \subset \{1, \dots, m\}$ such that*

$$V(x)_i = \tilde{V}(x_{k_{i,1}}, \dots, x_{k_{i,m}}), \quad \forall 1 \leq i \leq d. \quad (14)$$

Assumption 3 says that effectively, each component of the vector field V is a repeated instance of a lower dimensional functional unit \tilde{V} . Such vector fields occur in many natural complex phenomenon, such as networks of low dimensional dynamical systems (e.g. 28) and sub-grid modelling (e.g. 29; 30). A classic example is the Lorenz 96 model 19 we present later. Equation 14 provides the option of deriving the drift V as a low-dimensional conditional expectation problem. We now derive the precise nature of this expectation. For each $1 \leq i \leq d$, define projection maps

$$\pi_i : \mathbb{R}^d \rightarrow \mathbb{R}^{m+1}, \quad x \mapsto (x_{k_{i,1}}, \dots, x_{k_{i,m}}, x_i).$$

Define a measure $\tilde{\mu}$ on $\mathbb{R}^{m+1} = \mathbb{R}^m \times \mathbb{R}^m$ as follows :

$$\tilde{\mu}(A) := \mu \{x \in \mathbb{R}^d : \exists i \in \{1, \dots, d\} \text{ s.t. } \pi_i(x) \in A\}.$$

Thus $\tilde{\mu}$ is the sum of the push-forwards of the stationary measure μ along the projection maps π_i . We can now write

$$\tilde{V}(\tilde{x}) = \mathbb{E}_{\tilde{\nu}}(\tilde{Y} | \tilde{X} = \tilde{x}), \quad \forall \tilde{x} \in \mathbb{R}^m. \quad (15)$$

Equations 14 and (15) together present how V can be mined from high-dimensional data via conditional expectations. To utilize the relation in (15), we need the data to adhere to some requirements. A *causally complete snapshot* corresponding to a time instant t , an initial condition x_0 and a coordinate $i \in 1, \dots, d$ is a tuple

$$(X^{(i)}(t+3\Delta t, x_0), X^{(i)}(t+2\Delta t, x_0), X^{(i)}(t+\Delta t, x_0), X^{(i)}(t, x_0), \{X^{(j)}(t, x_0)\}_{j \in \text{Left}(i)}), \quad (16)$$

of length $m+1$.

Algorithm 3. *Drift estimation in a sparse SDE*

- **Input.**

- (i) An integer $m \leq d$ and for each $i \in \{1, \dots, d\}$ a collection of m coordinates $(k_{i,1}, \dots, k_{i,m}) \subset \{1, \dots, m\}$
- (ii) a collection of causally complete snapshots of the form (16), corresponding to various time instants t , index n , and an initial condition x_0 .

- **Parameters.** Same as Algorithm 1.

- **Output.** A matrix $A \in \mathbb{R}^{d \times M}$ such that

$$V(X) \approx \sum_{m=1}^M A_m k(x, x_m), \quad \forall x \in \mathbb{R}^d.$$

- **Steps.**

1. For each snapshot of the form (16), create a data-pair $(x_{t,i}, y_{t,i})$ such that

$$x_{t,i} = \{X^{(j)}(t, x_0)\}_{j \in \text{Left}(i)},$$

and

$$y_{t,i} = \frac{1}{\Delta t} [18X^{(i)}(t + \Delta t, x_0) - 9X^{(i)}(t + 2\Delta t, x_0) + 2X^{(i)}(t + 3\Delta t, x_0) - 11X^{(i)}(t, x_0)], \quad \forall n \in 1, \dots, N-$$

2. Pass the data set $\{(x_{t,i}, y_{t,i}) : t \geq 0, i \in 1, \dots, d\}$ to algorithm 1 along with the rest of parameters.
3. Store the result in a m -dimensional column vector $\tilde{a}^{(i)}$.
4. Compute the $d \times M$ matrix A such that

$$A^T = [\tilde{a}^{(1)}, \tilde{a}^{(2)}, \dots, \tilde{a}^{(d)}].$$

This completes the description of our algorithms. We apply this next to datasets collected from various SDEs.

(27)

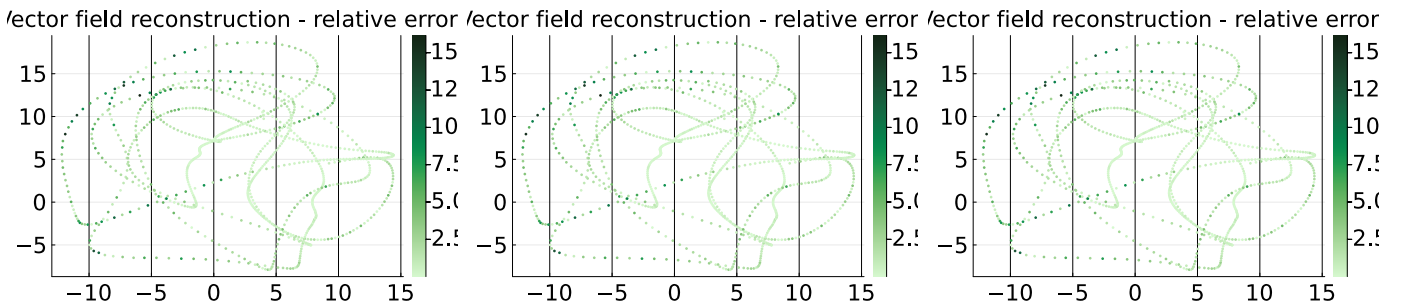


Figure 5: Error analysis for the Lorenz 96 system (19). The panels display the error in reconstructing the vector field at various points in the trajectory of the first cell.

4 Examples.

In this section we put to test our algorithms. We list the systems that we investigate :

Table 1: Summary of parameters in experiments. In all these experiments, the number of ...

System	properties	Figures	ODE Parameters	Data samples
Lorenz 63 (17)	Chaotic system in \mathbb{R}^3	2, 7	$\sigma = 10, \beta = 8/3,$ $\rho = 28$	10^4
Hopf oscillator (18)	Stable periodic cycle in \mathbb{R}^2	3, 6	$\mu = 1$	10^4
Lorenz 96 (19)	Chaotic system of 10 1-dimensional oscillators, cyclically coupled	5	$f = 8.0, N = 10$	2×10^3

Table 2: Auto-tuned parameters in experiments.

Ridge regression parameter δ	Bandwidth ϵ_1 of Gaussian kernel \mathcal{G}	Bandwidth ϵ_2 of RKHS kernel k	Bandwidth ϵ_3 of Markov kernel p
0.1	Chosen to achieve sparsity 0.3%	Chosen to achieve sparsity 1%	Chosen to achieve sparsity 1%

1. Lorenz 63.

$$\begin{aligned}
 \frac{d}{dt}x_1(t) &= \sigma(x_2 - x_1) \\
 \frac{d}{dt}x_2(t) &= x_1(\rho - x_3) - x_2 \\
 \frac{d}{dt}x_3(t) &= x_1x_2 - \beta x_3
 \end{aligned} \tag{17}$$

2. **Hopf oscillator.** The Hopf oscillator is used as a simple parametric model to study the phenomenon of Hopf bifurcations. Given a constant p , the ODE is

$$\begin{aligned}
 \frac{d}{dt}x_1(t) &= -x_2 + x_1(p - (x_1^2 + x_2^2)) \\
 \frac{d}{dt}x_2(t) &= x_1 + x_2(p - (x_1^2 + x_2^2))
 \end{aligned} \tag{18}$$

3. **Lorenz 96.** The Lorenz 96 model is a dynamical system formulated by Edward Lorenz in 1996

$$\frac{d}{dt}x_n(t) = (x_{n+1} - x_{n-2})x_{n-1} - x_n + F, \quad \forall n \in 1, \dots, N. \tag{19}$$

This model mimics the time evolution of an unspecified weather measurement collected at N equidistant grid points along a latitude circle of the earth (31). The constant F is known as the *forcing* function. The system (19) is benchmark problem in data assimilation.

The steps in each experiments were as follows :

1. The parameters for the ODEs were set according to Table 1.
2. The ODEs were converted into an SDE with the help of a diagonal diffusion term

$$G(x)_i = \sigma V(x)_i, \quad i = 1, \dots, d. \tag{20}$$

Table 3: Relative L^2 error in experiments

Experiment	Noise 0.1	Noise 0.2	Noise 0.5
Hopf oscillator (18)	0.02	0.03	0.06
Lorenz 63 (17)	0.08	0.1	0.14
Lorenz 96 (19) - 5 cells	0.31	0.27	0.265

3. The constant σ which controls the level of noise, was varied among the values $\{0.1, 0.2, 0.5\}$ respectively.
4. Algorithms 2 and 3 were applied as appropriate to a sample path of the SDE. The parameters for the algorithm were auto-tuned as described in Table 2.
5. The choice of kernel k was a diffusion kernel as in (21), and a Gaussian Markov normalized kernel as in (10).

Figure 1 represent some typical SDE orbits that we was provided as input to the algorithms. The results of the reconstruction have been displayed in Figures 3, 2, and 5 respectively. To further assess the accuracy of the methods, we compared the orbits generated by the true and estimated vector fields in Figures 6 and 7 respectively.

Choice of kernel. Our choice of kernel in all the experiments is the *diffusion* kernel (e.g. 32; 33). Among its various constructions, we choose the following :

$$k_{\text{diff},\epsilon}^\mu(x, y) = \frac{k_{\text{Gauss},\epsilon}(x, y)}{\text{deg}_l(x) \text{deg}_r(y)}, \quad (21)$$

$$\text{deg}_r(x) := \int_X k_{\text{Gauss},\epsilon}(x, y) d\mu(y), \quad \text{deg}_l(x) := \int_X k_{\text{Gauss},\epsilon}(x, y) \frac{1}{\text{deg}_r(x)} d\mu(y).$$

Diffusion kernels have been shown to be good approximants of the local geometry in various different situations (e.g. 34; 35; 36; 37), and are a natural choice for non-parametric learning. It has the added advantage of being symmetrizable :

$$\rho(x) k_{\text{diff},\epsilon}^\mu(x, y) \rho(y)^{-1} = \tilde{k}_{\text{diff},\epsilon}^\mu(x, y) = \frac{k_{\text{Gauss},\epsilon}(x, y)}{[\text{deg}_r(x) \text{deg}_r(y) \text{deg}_l(x) \text{deg}_l(y)]^{1/2}}, \quad (22)$$

where

$$\rho(z) = \text{deg}_l(z)^{1/2} / \text{deg}_r(z)^{1/2}.$$

The kernel $\tilde{k}_{\text{diff},\epsilon}^\mu$ from (22) is clearly symmetric. Since it is built from the s.p.d. kernel $k_{\text{Gauss},\epsilon}$, $\tilde{k}_{\text{diff},\epsilon}^\mu$ is s.p.d. too and thus generates an RKHS of its own. Moreover, the kernel $k_{\text{diff},\epsilon}^\mu$ can be symmetrized by a degree function ρ , which is both bounded and bounded above 0. Such a kernel will be called *RKHS-like*. Let M_ρ be the multiplication operator with ρ . Then

$$\text{ran } K_{\text{diff},\epsilon}^\mu = \text{ran } M_\rho \circ \tilde{K}_{\text{diff},\epsilon}^\mu.$$

Again, because of the properties of ρ , both M_ρ and its inverse are bounded operators. Thus there is a bijection between the RKHS generated by $\tilde{k}_{\text{diff},\epsilon}^\mu$, and the range of the integral operator $K_{\text{diff},\epsilon}^\mu$.

Bandwidth selection. We now present our method of selecting a bandwidth ϵ for constructing a kernel over a dataset \mathcal{D} . It depends on the choice of a threshold $\eta \in (0, 1)$, and a zero threshold $\theta_{\text{zero}} = 10^{-14}$.

We first choose a subsample \mathcal{D}' of the data set \mathcal{D} and construct the set \mathcal{S} of all possible pairwise squared distances. Usually, it suffices to choose \mathcal{D}' to be 0.1 fraction of the dataset \mathcal{D} , equidistributed throughout \mathcal{D} . Now set another threshold :

$$\theta = -1/\ln(\theta_{zero}).$$

Given the η , we set ϵ such that η -fraction of the numbers in \mathcal{S} are less than θ . In other words, with this choice of ϵ , an η fraction of the set $\{e^{-\|x-x'\|^2/\epsilon} : x, x' \in \mathcal{D}'\}$ are greater than θ_{zero} .

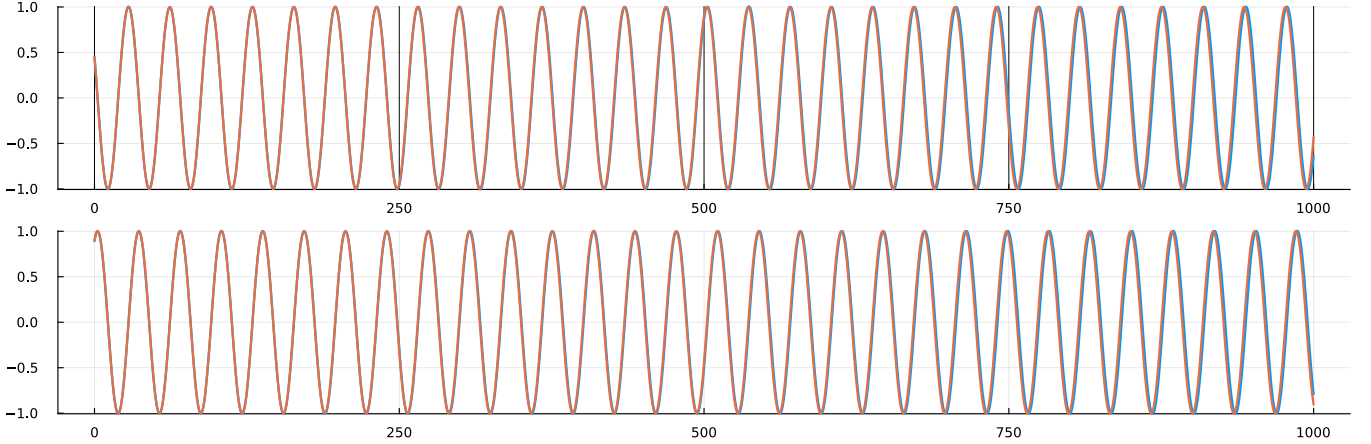


Figure 6: Reconstruction of the Hopf oscillator

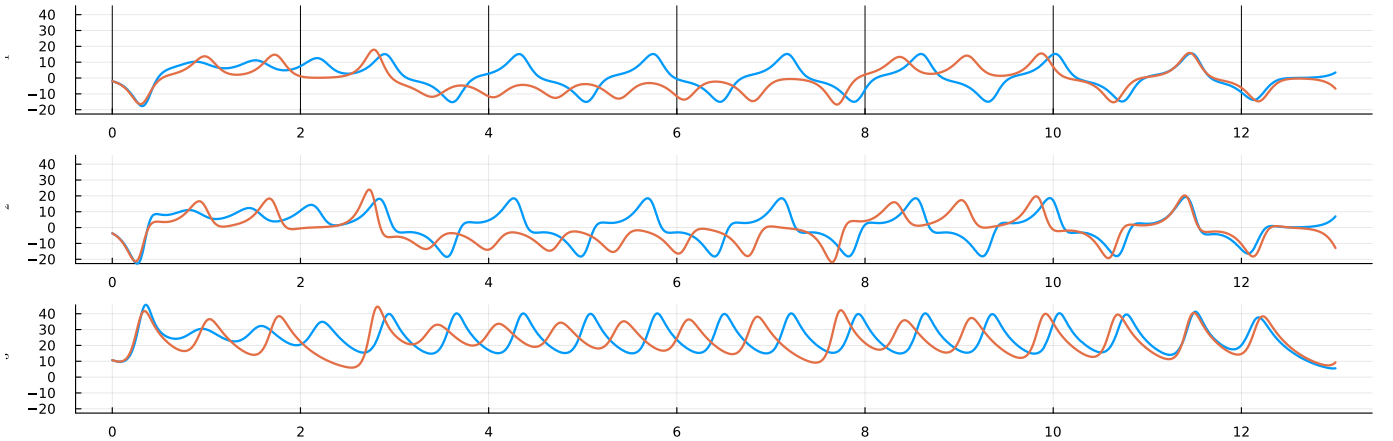


Figure 7: Reconstruction of the Lorenz 63 system

Evaluating the results. There is no certain way of evaluating the efficacy of a reconstruction technique for chaotic systems, as argued in (38). In any data-driven approach such as ours, the reconstruction is done in dimensions higher than the original system. As a result, new directions of instability are introduced, and even if the vector field is reconstructed with good precision, the results of their simulation might be completely different. For that purpose, our primary means of evaluating the accuracy of our vector field reconstruction is by a pointwise evaluation of the reconstruction error, as shown in Figures 2, 3 and 4. The average errors are tabulated in Table 3. Also see Figures 6, 7, 8 and 9 for a comparison of orbits from the true system and the reconstructed system. It can be noted in the last two figures that the orbits of the reconstructed system get stuck in a false fixed point. This is an artefact of the technique of making out of sample evaluations, which we discuss next.

L96, N=5, noise=0.1

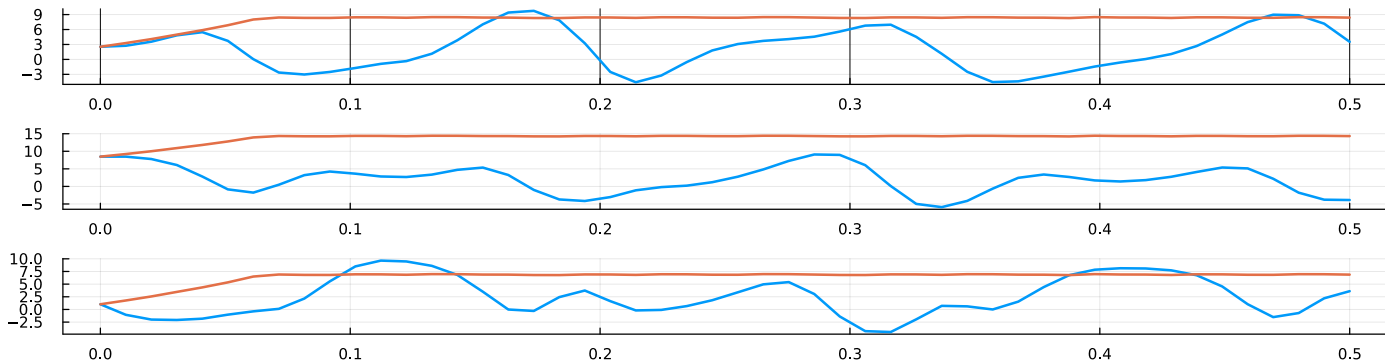


Figure 8: Reconstruction of the Lorenz 96 system with 5 cells. The orbits of the true and reconstructed systems diverge rapidly due to the presence of positive Lyapunov exponents in the L96 system. See Figure 9 for a closer look at the plots.

L96, N=5, noise=0.1

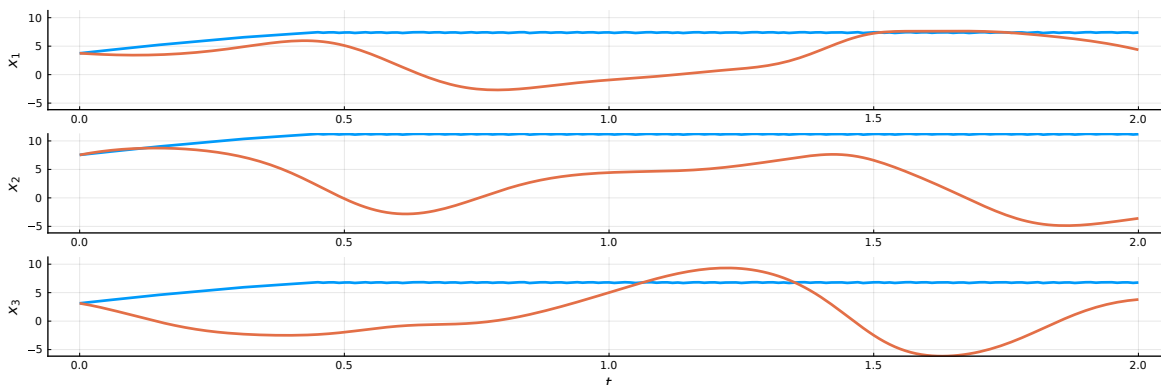


Figure 9: Reconstruction of the Lorenz 96 system with 5 cells. This figure offers a closer look at the graphs of Figure 8.

Evaluating kernel functions. Any kernel function $\phi(x) = \sum_{n=1}^N k(x, x_n)$ created from a diffusion kernel (21) can be evaluated at an arbitrary point x in \mathbb{R}^d as

$$\phi(x) = \frac{1}{N} [\bar{\rho}_l(x) \bar{\rho}_r(x)]^{-0.5} \sum_{n=1}^N k_{Gauss, \epsilon}(x, x_n) w_n,$$

where the other terms are given by

$$w_n = [\text{deg}_r(x_n) \text{deg}_l(x_n)]^{-0.5}, \quad \bar{\rho}_r(x) = \frac{1}{N} \sum_{n=1}^N k_{Gauss, \epsilon}(x, x_n), \quad \bar{\rho}_l(x) = \frac{1}{N} \sum_{n=1}^N k_{Gauss, \epsilon}(x, x_n) / \text{deg}_r(x_n).$$

Note that the vector $\vec{w} = (w_1, \dots, w_N)$ is independent of x and is computed during the creation of the kernel matrix. While the computation is straightforward, a numerical issue arises when the test point x is far from the data set $\{x_n : n \in 1, \dots, N\}$. In that case, the vector $(k_{Gauss, \epsilon}(x, x_n))_{n=1}^N$ have all entries below the machine precision. As a result the constant $\bar{\rho}_r(x)$ is also below machine precision. The occurrence of such near-zero numbers could lead to several computational anomalies. We use a nearest point approximation for evaluating the kernel sum in such cases. This also leads to false fixed points emerging at locations far from the dataset. We discuss this issue more in our concluding section.

5 Conclusions.

We have thus described a simple numerical method based on a sound mathematical principle, which can estimate drift from timeseries generated by SDEs. It worked well for the chaotic and quasiperiodic systems of dimensions less than six that we investigated. The performance deteriorates as the dimension increases.

Choice of parameters. The three main tuning parameters in our algorithm are the Ridge regression δ and kernel bandwidth parameters $\epsilon_1, \epsilon_2, \epsilon_3$. Among these, the most important is the smoothing parameter ϵ_3 which determines the effective radius of integration. The smaller ϵ_3 is, the higher the number N of total samples has to be. Thus a larger smoothing radius ϵ_3 leads to a faster convergence with N . On the other hand, a larger ϵ_3 and N also increases the condition number of the Markov matrix $[P]$, which could adversely affect the accuracy of the solution to the linear least squares problem (12). There is no recipe for tuning these parameters that would work uniformly well in all applications.

Choice of kernel. Note that Algorithm 1 does not specify the kernel, and any RKHS-like kernel such as the diffusion kernel would be sufficient. The convergence laid down in Lemma 2.1 also does not depend on the choice of kernel. However when finite data is used, the choice of kernel becomes important. The question of an optimal kernel is an important and unsolved question in machine learning (e.g. 39; 40; 41). Our framework for estimating drift provides a more objective setting for this question.

Networked dynamical systems. One of the extensions of our technique was for high dimensional systems with sparsity, as described in Section 3. One of the most important examples of such systems are networked dynamical systems. The description of such systems involve (i) a vector field governing the dynamics of each cell; (ii) an adjacency matrix \mathbb{A} describing the coupling between cells. Another future direction of research is to devise a similarity transform on \mathbb{A} which creates a sparse matrix. Then the techniques of Algorithm 3 would become applicable.

Out-of-sample extensions. The technique that we presented provides a robust estimation technique for the drift. The reason it is well suited to a general nonlinear and data-driven technique is the use of kernel methods. The downside of kernel methods is the difficulty in extending the function beyond the compactly supported dataset. Thus our technique provides a good phase-portrait, but it may not be reliable as a simulator or alternative model to the true system if the latter is chaotic and high dimensional. The issue of out of sample extensions (e.g. 42; 43) and topological containment (e.g. 44; 45) of simulation models is separate from the preliminary task of estimating the vector field close to the system. This is yet another important area of development.

References.

- [1] L. Arnold. *Stochastic differential equations : theory and applications*. Wiley Interscience, 1974.
- [2] F. Philipp, M. Schaller, K. Worthmann, S. Peitz, and F. Nüske. [Error bounds for kernel-based approximations of the Koopman operator](#), 2023.
- [3] C. Shalizi and A. Kontorovich. *Almost none of the theory of stochastic processes*. Lecture Notes, 2010.
- [4] R. Stanton. [A nonparametric model of term structure dynamics and the market price of interest rate risk](#). *J. Finance*, 52(5):1973–2002, 1997.
- [5] G Gouesbet. [Reconstruction of the vector fields of continuous dynamical systems from numerical scalar time series](#). *Physical Review A*, 43(10):5321, 1991.

- [6] N. Tsutsumi, K. Nakai, and Y. Saiki. [Constructing differential equations using only a scalar time-series about continuous time chaotic dynamics](#). *Chaos*, 32(9), 2022.
- [7] G Gouesbet and Christophe Letellier. [Global vector-field reconstruction by using a multivariate polynomial 1 2 approximation on nets](#). *Physical Review E*, 49(6):4955, 1994.
- [8] J Cao, L Wang, and J Xu. [Robust estimation for ordinary differential equation models](#). *Biometrics*, 67(4):1305–1313, 2011.
- [9] Y. Aït-Sahalia, L. Hansen, and J. Scheinkman. Operator methods for continuous-time Markov processes. In *Handbook of financial econometrics: tools and techniques*, pages 1–66. Elsevier, 2010.
- [10] S. Siegert, R. Friedrich, and J. Peinke. [Analysis of data sets of stochastic systems](#). *Phys. Lett. A*, 243(5-6):275–280, 1998.
- [11] J. Gradišek et al. [Analysis of time series from stochastic processes](#). *Phys. Rev. E*, 62(3):3146, 2000.
- [12] R. Friedrich et al. [Extracting model equations from experimental data](#). *Phys. Lett. A*, 271(3):217–222, 2000.
- [13] A. Ruttor, P. Batz, and M. Opper. [Approximate gaussian process inference for the drift function in stochastic differential equations](#). *Adv. Neural Inf. Processing Sys.*, 26, 2013.
- [14] S. Das. [Conditional expectation using compactification operators](#). *Appl. Comput. Harmon. Anal.*, 71:101638, 2024.
- [15] R. Sechi, A. Sikorski, and M. Weber. [Estimation of the Koopman generator by Newton’s extrapolation](#). *Multiscale Modeling & Simulation*, 19(2):758–774, 2021.
- [16] P. Sura and J. Barsugli. [A note on estimating drift and diffusion parameters from timeseries](#). *Phys. Lett. A*, 305(5):304–311, 2002.
- [17] R. Friedrich, J. Peinke, and C. Renner. [How to quantify deterministic and random influences on the statistics of the foreign exchange market](#). *Phys. Rev. Lett.*, 84(22):5224, 2000.
- [18] G. Banon. [Nonparametric identification for diffusion processes](#). *SIAM J. Control and Optimization*, 16(3):380–395, 1978.
- [19] S. Das and D. Giannakis. [Delay-coordinate maps and the spectra of Koopman operators](#). *J. Stat. Phys.*, 175:1107–1145, 2019.
- [20] S. Das and D. Giannakis. [Koopman spectra in reproducing kernel Hilbert spaces](#). *Appl. Comput. Harmon. Anal.*, 49:573–607, 2020.
- [21] D. Giannakis and S. Das. [Extraction and prediction of coherent patterns in incompressible flows through space-time Koopman analysis](#). *Phys. D*, 402:132211, 2019.
- [22] S. Das, D. Giannakis, and E. Szekeley. [An information-geometric approach for feature extraction in ergodic dynamical systems](#), 2020.
- [23] S. Mustavee, S. Das, and S. Agarwal. [Data-driven discovery of quasiperiodically driven dynamics](#), 2023.
- [24] S. Das, S. Mustavee, S. Agarwal, and S. Hassan. [Koopman-theoretic modeling of quasiperiodically driven systems: Example of signalized traffic corridor](#). *IEEE Trans. SMC Sys.*, 53:4466–4476, 2023.

- [25] D. Giannakis, S. Das, and J. Slawinska. [Reproducing kernel Hilbert space compactification of unitary evolution groups](#). *Appl. Comput. Harmon. Anal.*, 54:75–136, 2021.
- [26] V. Paulsen. [An introduction to the theory of reproducing kernel Hilbert spaces](#), 2016.
- [27] R. Gonzalez. *Digital image processing*. Pearson education india, 2009.
- [28] CL. Yang and C. Suh. [On controlling dynamic complex networks](#). *Physica D*, 441:133499, 2022.
- [29] Y. Guan et al. [Learning physics-constrained subgrid-scale closures in the small-data regime for stable and accurate les](#). *Physica D*, 443:133568, 2023.
- [30] D. Boutros and E. Titi. [Onsager’s conjecture for subgrid scale \$\alpha\$ -models of turbulence](#). *Physica D*, 443:133553, 2023.
- [31] E. Lorenz and K. Emanuel. [Optimal sites for supplementary weather observations: Simulation with a small model](#). *Journal of the Atmospheric Sciences*, 55(3):399–414, 1998.
- [32] N. Marshall and R. Coifman. [Manifold learning with bi-stochastic kernels](#). *IMA J. Appl. Math.*, 84(3):455–482, 2019.
- [33] C. Wormell and S. Reich. [Spectral convergence of diffusion maps: Improved error bounds and an alternative normalization](#). *SIAM J. Numer. Anal.*, 59(3):1687–1734, 2021.
- [34] T. Berry, S. Das, D. Giannakis, and R. Vaughn. [Spectral convergence of kernel integral operators](#), 2021. in preparation.
- [35] R Coifman and S Lafon. [Diffusion maps](#). *Appl. Comput. Harmon. Anal.*, 21:5–30, 2006.
- [36] M. Hein, JY. Audibert, and U. Von Luxburg. [From graphs to manifolds—weak and strong pointwise consistency of graph Laplacians](#). In *International Conference on Computational Learning Theory*, pages 470–485. Springer, 2005.
- [37] R. Vaughn, T. Berry, and H. Antil. [Diffusion maps for embedded manifolds with boundary with applications to pdes](#). *Appl. Comput. Harmonic Anal.*, 68:101593, 2024.
- [38] T. Berry and S. Das. [Learning theory for dynamical systems](#). *SIAM J. Appl. Dyn.*, 22:2082 – 2122, 2023.
- [39] A. Narayan, L. Yan, and T. Zhou. [Optimal design for kernel interpolation: Applications to uncertainty quantification](#). *J. Comput. Phys.*, 430:110094, 2021.
- [40] R. Baraniuk and D. Jones. [A signal-dependent time-frequency representation: optimal kernel design](#). *IEEE Trans. Signal Process.*, 41(4):1589–1602, 1993.
- [41] K. Crammer, J. Keshet, and Y. Singer. [Kernel design using boosting](#). *Adv. Neural Inf Process. Sys.*, 15, 2002.
- [42] E. Vural and C. Guillemot. [Out-of-sample generalizations for supervised manifold learning for classification](#). *IEEE Trans. Image Processing*, 25(3):1410–1424, 2016.
- [43] B. Pan et al. [Out-of-sample extensions for non-parametric kernel methods](#). *IEEE Trans. neural netw. learning sys.*, 28(2):334–345, 2016.
- [44] T. Kaczynski, M. Mrozek, and T. Wanner. [Towards a formal tie between combinatorial and classical vector field dynamics](#). *J. Computational Dynamics*, 3(1):17–50, 2016.

- [45] M. Mrozek and T. Wanner. [Creating semiflows on simplicial complexes from combinatorial vector fields](#). *J. Dif. Eq.*, 304:375–434, 2021.